L. J. SCERBO
D. L. POPE
Bell Telephone Laboratories,
Whippany, N. J.

Bounding Solutions for Performance of Vibratory Plows

This paper discusses the reduction in the applied drawbar force required to penetrate soil with vibrating plows. Harmonically forced linear and orbital motions of a plow blade are investigated. A rigid blade, vibrating with constant amplitude and a two-parameter soil model is used to represent the system. The assumption that the soil force opposes the instantaneous blade velocity vector is sufficient to describe the soil-blade interaction. Bounding solutions, which relate applied drawbar force to average plowing speed and other system parameters, are obtained as simple equations. These equations put into perspective the relative merits of each of these vibratory motions.

Introduction

INERTIAL actuators driven by one or several eccentric weights are now being used in vibrating plows. These plows provide a temporary slit in the earth for the out-of-sight installation of various utilities. They offer an economical and ecologically attractive alternative to other methods of direct burial.

During the past few years, many investigators have documented the effect of vibration on reducing the average required drawbar force to penetrate earth. Senator [1],[1] Nalezny, and Boyd [2] have shown analytically and experimentally that the magnitude of the reduction depends on (*a*) mode of plow blade vibration; (*b*) dimensionless ratio of the average drawbar force ($\bar{P}$) to the static soil strength (P_0), called $\hat{p}$; (*c*) dimensionless ratio of average penetration rate ($\dot{x}$) to the maximum plow blade vibrational velocity ($a\Omega$), called $\hat{v}$; and (*d*) the fraction of soil resistance that can be attributed to friction, denoted by γ. The soil model used by each of these investigators is different. Each author, however, uses a horizontal momentum balance to derive his results. The horizontal component of the instantaneous force, ($P(t)$), acting on the blade is integrated over a cycle and equated to the average drawbar force ($\bar{P}$) acting for the duration of the cycle.

$$\int_0^{2\pi/\Omega} P(t) \cos \beta \, dt = \frac{2\pi}{\Omega} \bar{P} \qquad (1)$$

This paper presents an analysis of the expected reduction in the average drawbar force required to penetrate soil with vibrating plows based on equation (1). Results are presented in terms of simple bounding equations. The pertinent relationships are not hidden beneath a mass of complicated integrals and pages of parametric plots. The bounding equations put into perspective the relative merits of the different modes of vibration presently popular, and are substantiated by agreement with available experimental field data. These equations are also useful to estimate penetration rates for existing and conceptual plow designs and can be used to study the optimum choices for system parameters.

This paper develops approximate solutions for the $\hat{p}$ versus $\hat{v}$ relationship for both orbital and linear harmonic motions of a plow blade. The solutions are valid for $0 < \hat{v} < 0.2$ and are carried out including all terms of order $\hat{v}^2$. This range of the nondimensional penetration rate, $\hat{v}$, includes most situations of practical interest. The analyses are based on the simple assumption that the direction of the soil force acting on the blade opposes the instantaneous blade velocity vector.

The soil model assumed for this work is a simple, two-parameter, Coulomb friction model. A force, P_0, represents the static resistance of uncut soil to penetration by the plow blade. This force includes the strength of the virgin soil as well as the frictional resistance to the forward advance of the blade. In certain modes of vibratory soil penetration, however, during a portion of the cycle the plow blade moves through previously cut soil. During this interval, the forces on the blade are assumed to be due entirely to the frictional resistance of the soil. This frictional resistance is characterized by a parameter γ which represents the fraction of the static soil resistance P_0 attributable to friction. In practice, γ varies between zero and unity.

Bounding solutions for the relationship between drawbar force and penetration rate are established by considering the cases $\gamma = 0$ and $\gamma = 1$, respectively. When $\gamma = 0$, the resistance to blade motion is associated totally with the static strength of uncut soil. This is the "all tip resistance" case and generally establishes an upper bound for the $\hat{p}$ versus $\hat{v}$ relation. On the other hand, if $\gamma = 1$, friction is the dominant factor in the forces on the blade. This situation is the "all skin friction" case and represents lower bound for the $\hat{p}$ versus $\hat{v}$ relationship.

---

[1] Numbers in brackets designate References at end of paper.

Contributed by the Vibration and Sound Committee of the Design Engineering Division of THE AMERICAN SOCIETY OF MECHANICAL ENGINEERS and presented at the Design Engineering Technical Conference, Cincinnati, Ohio, September 9–12, 1973. Manuscript received at ASME Headquarters June 6, 1973. Paper No. 73-DET-128.

This simple, two-parameter, Coulomb friction soil model permits analyses of various modes of vibratory soil penetration to be carried out and yields qualitatively respectable results. No consideration is given in this analysis to additional soil parameters such as moisture content, density, viscosity, or other effects, such as the blade geometry, which are known to influence the performance of vibratory soil-penetrating equipment.

Analysis for Orbital Motion

The analytical model for the orbital case further assumes steady state conditions and a rigid blade with infinite harmonic shaking force. Thus, all points on the blade move on a circular path of radius a, and the angular velocity of the circular motion, Ω, is constant. The force acting on the blade is either P_0 or γP_0, depending on the position of the blade in the orbit.

Fig. 1 represents the assumption that the instantaneous soil force opposes the instantaneous blade velocity vector. We first consider the effect of the inclination of the instantaneous velocity vector. From Fig. 1,

$$\cos \beta = \frac{\dot{x} - a\Omega \sin \theta}{[(\dot{x} - a\Omega \sin \theta)^2 + (a\Omega \cos \theta)^2]^{1/2}} \tag{2}$$

Rearranging, we obtain

$$\cos \beta = \frac{\hat{v} - \sin \theta}{[1 + \hat{v}^2 - 2\hat{v} \sin \theta]^{1/2}} \tag{3}$$

The horizontal component of the instantaneous force on the blade by definition is either

$$(P_0 \quad \text{or} \quad \gamma P_0) \cdot \cos \beta \tag{4}$$

The integral of this expression, as required in equation (1), is not available in closed form. To approximate this integral, we first develop a Taylor series expansion for the integrand about the point $\hat{v} = 0$.

$$[1 + \hat{v}^2 - 2\hat{v} \sin \theta]^{-1/2} \simeq 1 + \hat{v} \sin \theta + \frac{\hat{v}^2}{2}(3 \sin^2 \theta - 1) + \ldots \tag{5}$$

Thus,

$$\cos \beta = \frac{\hat{v} - \sin \theta}{[1 + \hat{v}^2 - 2\hat{v} \sin \theta]^{1/2}}$$

$$\simeq -\sin \theta + \hat{v} \cos^2 \theta + \frac{3}{2}\hat{v}^2 \sin \theta \cos^2 \theta + \ldots \tag{6}$$

Only the terms up to and including the second order in $\hat{v}$ are retained.

We now must determine the intervals of the orbit during which P_0 and γP_0 act. Fig. 2 shows conditions during a typical orbit and helps define the switching angles α and ϕ. As shown, α is the switching angle at which the blade leaves previously uncut soil and $P(t)$ changes from P_0 to γP_0; and ϕ is the switching angle at which the blade first encounters uncut soil where $P(t)$ changes

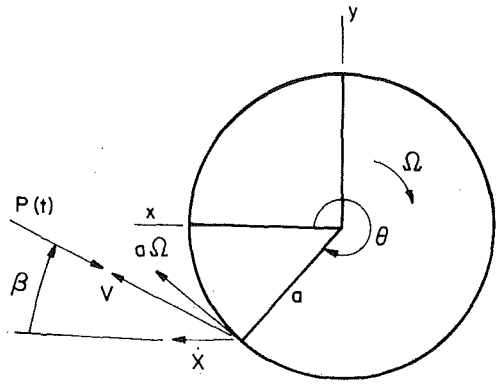

Fig. 1 Instantaneous soil force $P(t)$ opposes the instantaneous blade velocity vector V

from γP_0 to P_0. The total advance of the blade during a cycle is equal to the sum of the horizontal displacement of the blade relative to the center of rotation, pt. 0, during penetration of uncut soil and the displacement of the center of rotation during the time the blade is moving through uncut soil. The advance per cycle is also equal to the average horizontal velocity times the period of the motion, by definition.

$$\dot{x} \cdot \frac{2\pi}{\Omega} = a \cos \alpha - a \cos \phi + \dot{x} \frac{(\alpha + \phi)}{\Omega} \tag{7}$$

The switching angle α at which the blade leaves previously uncut soil is determined by the equation

$$a\Omega \sin \alpha = \dot{x} \tag{8}$$

These equations can be written in dimensionless form,

$$\sin \alpha = \hat{v}$$
$$\cos \alpha = (1 - \hat{v}^2)^{1/2} \tag{9}$$

and

$$\cos \phi = \hat{v}\alpha + \cos \alpha - \hat{v}(2\pi - \phi) \tag{10}$$

In terms of these switching angles, equation (1) becomes

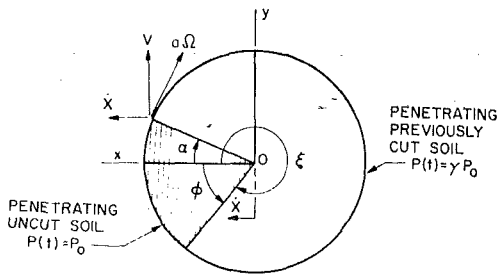

Fig. 2 Conditions during a typical cycle

Nomenclature

$P(t)$ = instantaneous soil force acting on the blade
P_0 = soil force acting on the blade during motion through previously uncut soil
γP_0 = soil force acting on the blade during motion through previously cut soil
$\bar{P}$ = average drawbar force during one cycle
$\hat{p}$ = nondimensional bias force = $\bar{P}/P_0$
$\dot{x}$ = average horizontal velocity
a = maximum amplitude of plow blade oscillation
Ω = frequency of blade oscillation
$\hat{v}$ = nondimensional penetration rate = $\dot{x}/a\Omega$
β = angle between soil force vector and horizontal
γ = coulomb friction reduction factor
α = switching angle at which blade leaves uncut soil and $P(t)$ changes from P_0 to γP_0
ϕ = switching angle at which blade first contacts uncut soil and $P(t)$ changes from γP_0 to P_0

$$P_0 \int_0^{\alpha} \cos \beta d\theta + \gamma P_0 \int_{\alpha}^{\xi} \cos \beta d\theta + P_0 \int_{\xi}^{2\pi} \cos \beta d\theta = 2\pi \bar{P} \tag{11}$$

From equation (6) we have:

$$\int_A^B \cos \beta d\theta \simeq \cos \theta + \frac{\hat{v}}{2} (\theta + \sin \theta \cos \theta) - \frac{1}{2} \hat{v}^2 \cos^3 \theta \Big|_A^B \tag{12}$$

Evaluating equation (11) with the indicated limits, we obtain:

$$\begin{aligned} P_0 &\left\{ \cos \alpha + \frac{\hat{v}}{2} (\alpha + \sin \alpha \cos \alpha) - \frac{1}{2} \hat{v}^2 \cos^3 \alpha - 1 + \frac{1}{2} \hat{v}^2 \right\} \\ &- \gamma P_0 \left\{ (\cos \alpha - \cos \xi) + \frac{\hat{v}}{2} (\alpha - \xi + \sin \alpha \cos \alpha \right. \\ &\left. - \sin \xi \cos \xi) - \frac{1}{2} \hat{v}^2 (\cos^3 \alpha - \cos^3 \xi) \right\} \\ &+ P_0 \left\{ 1 + \pi \hat{v} - \frac{1}{2} \hat{v}^2 - \cos \xi - \frac{\hat{v}}{2} (\xi + \cos \xi \sin \xi) \right. \\ &\left. + \frac{1}{2} \hat{v}^2 \cos^3 \xi \right\} = 2\pi \bar{P} \end{aligned} \tag{13}$$

Combining terms, we have:

$$\begin{aligned} P_0(1 - \gamma) &\left\{ (\cos \alpha - \cos \xi) + \frac{\hat{v}}{2} \right. \\ &\times (\alpha - \xi + \sin \alpha \cos \alpha - \sin \xi \cos \xi) \\ &\left. - \frac{1}{2} \hat{v}^2 (\cos^3 \alpha - \cos^3 \xi) \right\} + \hat{v} \pi P_0 = 2\pi \bar{P} \end{aligned} \tag{14}$$

We now express this relationship in terms of the acute angles α and ϕ shown in Fig. 2.

$$\begin{aligned} P_0(1 - \gamma) &\left\{ (\cos \alpha - \cos \phi) + \frac{\hat{v}}{2} \right. \\ &\times (\alpha + \phi - 2\pi + \sin \alpha \cos \alpha + \sin \phi \cos \phi) \\ &\left. - \frac{1}{2} \hat{v}^2 (\cos^3 \alpha - \cos^3 \phi) \right\} + \hat{v} \pi P_0 = 2\pi \bar{P} \end{aligned} \tag{15}$$

The switching angle relationships, equations (9) and (10), permit us to express all the factors in equation (15) in terms of the nondimensional penetration rate, $\hat{v}$. First of all, from equation (9),

$$\sin \alpha = \hat{v} \tag{16}$$

$$\cos \alpha = \sqrt{1 - \hat{v}^2} = 1 - \frac{1}{2} \hat{v}^2 + 0(\hat{v}^4) \tag{17}$$

$$\alpha = \hat{v} + 0(\hat{v}^3) \tag{18}$$

Equation (10) is a transcendental equation for ϕ. A solution to this equation, valid to $0(\hat{v}^2)$, is developed in the Appendix. In terms of an auxiliary variable z, we find

$$\sin \phi = 2z - \frac{1}{\pi} z^2 - z^3 + \frac{4}{3\pi} z^4 \quad \ldots \tag{19}$$

$$\cos \phi = 1 - 2z^2 + \frac{2}{\pi} z^3 - \frac{1}{2\pi^2} z^4 \quad \ldots \tag{20}$$

$$\phi = 2z - \frac{1}{\pi} z^2 + \frac{1}{3} z^3 - \frac{2}{3\pi} z^4 \quad \ldots \tag{21}$$

where

$$z = \sqrt{\pi \hat{v}} \tag{22}$$

Note that for consistent ordering of terms, factors up to and including the fourth power in z must be retained.

We now substitute these expressions into equation (15). The results, after some manipulation, are

$$P_0(1 - \gamma)\{z^2 + 0(z^5)\} + z^2 P_0 = 2\pi \bar{P} \tag{23}$$

or

$$\bar{P}/P_0 = \hat{p} \simeq \frac{\hat{v}}{2} (2 - \gamma) \tag{24}$$

Note that, even though equation (24) contains only a single first-order term in $\hat{v}$, it is accurate to a higher order. The second-order term in the equation vanishes, so the first possible nonzero higher order term is of order $(\hat{v})^{5/2}$. This suggests that the relationship given by equation (24) is good to within at least 3 percent for values of $\hat{v}$ as large as 0.2. This is certainly well within the accuracy of the modeling.

To obtain the bounding solutions for the orbital analysis, γ is set equal to one and then zero. When $\gamma = 1$, we have the "all skin friction" case and equation (24) becomes simply

$$\hat{p} \simeq \frac{\hat{v}}{2} \tag{25}$$

and a lower bound is obtained.

The slope of the $\hat{p}$ versus $\hat{v}$ curve for $\gamma \neq 1$ is steeper than for $\gamma = 1$. The steepest slope occurs when $\gamma = 0$. This situation corresponds to the "all tip resistance" case, and the upper bound,

$$\hat{p} = \hat{v} \tag{26}$$

Fig. 3 gives the two bounding $\hat{p}$ versus $\hat{v}$ curves for the orbital case. Fig. 3 also includes preliminary results from an experimental field test program with an orbital plow performed at Bell Laboratories [3]. Results fall nicely within the bounds given by this analysis. They also seem to indicate a definite trend toward the "all skin friction" model.

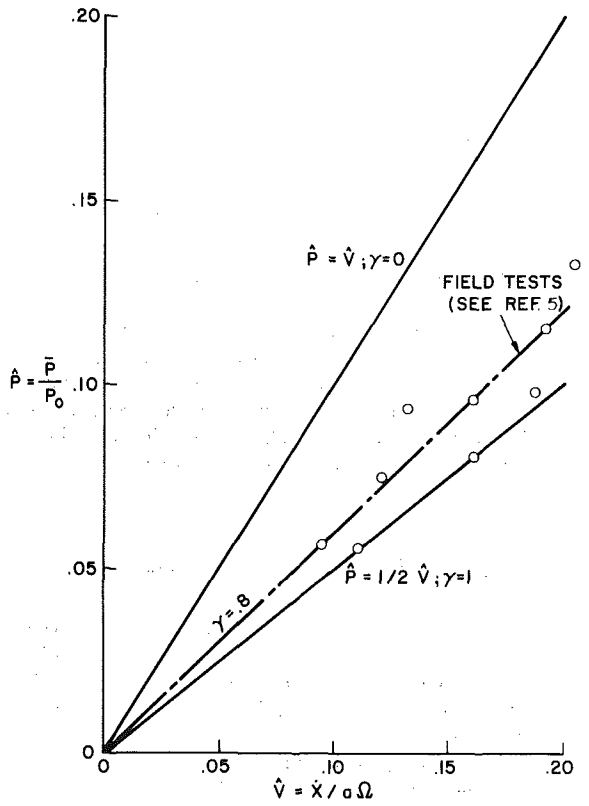

Fig. 3 Bounding solutions and experimental field data for orbital vibration

Analysis for Linear Harmonic Motion

The linear harmonic analysis considers two cases, vertical vibration and fore-aft vibration of the plow blade. These are the most widely used modes of plow blade vibration and represent the extremes of a general linear harmonic analysis. The results for the general case, in which the axis of vibration is inclined at an angle ψ to the vertical, must be obtained numerically for $0 < \psi < 90$ deg. The solutions for the general case are bounded by the results for the vertical and fore-aft cases, so will not be presented in detail. One result for $\psi = 40$ deg and $\gamma = 1$ is shown, however, for comparison.

The harmonic analysis further assumes steady-state conditions, a constant frequency of vibration (Ω), and a nonvarying sinusoidal amplitude, a, of plow blade vibration.

Fore-Aft Case. For the fore-aft vibrating case, $\psi = 90$ deg, and $\cos\beta$ is either ($\pm$) unity. Therefore, to integrate equation (1) we need only to determine the intervals of the cycle during which P_0 or γP_0 act. It is evident that the transcendental relation given by equation (7) also applies to the fore-aft case,

$$\dot{x}\cdot\frac{2\pi}{\Omega} = a\cos\alpha - a\cos\phi + \dot{x}\frac{(\alpha+\phi)}{\Omega}$$

where α and ϕ define the same switching angles. From a sketch similar to Fig. 2 for fore-aft vibration, it is clear that the plow begins to move forward again at an angle $\theta = \pi - \alpha$.

In terms of these switching angles the horizontal momentum balance equation is,

$$\int_0^{\alpha} P_0 d\theta - \int_{\alpha}^{\pi-\alpha} \gamma P_0 d\theta + \int_{\pi-\alpha}^{2\pi-\phi} \gamma P_0 d\theta + \int_{2\pi-\phi}^{2\pi} P_0 d\theta = \int_0^{2\pi} \bar{P} d\theta \quad (27)$$

Evaluating these integrals we obtain:

$$P_0(\alpha+\phi) + \gamma P_0(3\alpha - \phi) = \bar{P}(2\pi) \quad (28)$$

or

$$(\alpha+\phi) + \gamma(3\alpha - \phi) = \hat{p}(2\pi) \quad (29)$$

This equation can be further simplified if the discussion is limited to small $\hat{v}$. From the relation given in equation (18),

$$\alpha \simeq \hat{v}$$

and

$$\phi \simeq (2\sqrt{\pi\hat{v}} - \hat{v} + \pi\hat{v}\sqrt{\pi\hat{v}}/3 - 2\pi\hat{v}^2/3 + \ldots)^2$$

Making these substitutions, we obtain

$$\hat{p} \simeq \left(\sqrt{\frac{\hat{v}}{\pi}} + \pi\hat{v}\sqrt{\frac{\hat{v}}{\pi}}\Big/6 - \hat{v}^2/3\right) + \gamma\left(2\hat{v}/\pi - \sqrt{\frac{\hat{v}}{\pi}} - \pi\hat{v}\sqrt{\frac{\hat{v}}{\pi}}\Big/6 + \hat{v}^2/3\right) \quad (30)$$

For the "all skin friction" case, ($\gamma = 1$), this equation reduces to

$$\hat{p} \simeq \frac{2\hat{v}}{\pi},$$

the lower bound.

The upper bound for the fore-aft case is obtained for the "all tip resistance" case, ($\gamma = 0$). In this case the solution up to second order is given by

$$\hat{p} \simeq (1 + \pi\hat{v}/6)\sqrt{\frac{\hat{v}}{\pi}}$$

[2] See Appendix.

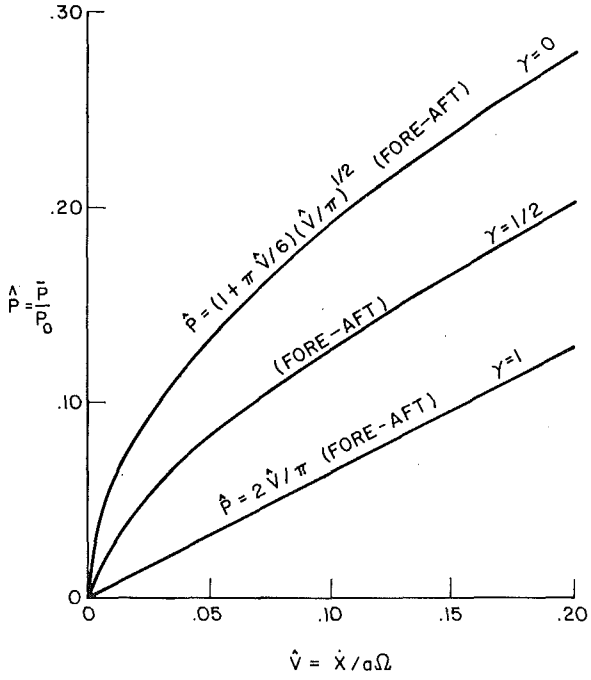

Fig. 4 Fore-aft analytic predictions — various γ

These results and an intermediate relationship for $\gamma = 1/2$ are plotted in Fig. 4.

Vertical Case

When $\psi = 0$ deg, the harmonic motion of the blade takes place along a vertical line. The blade never loses contact with uncut soil. This condition requires a somewhat different interpretation of the Coulomb soil model. The horizontal momentum balance equation, (equation (1)), is now written as

$$2\pi(1-\gamma)P_0 + \gamma P_0 \int_0^{2\pi} \frac{\dot{x}}{\sqrt{\dot{x}^2 + (a\Omega\cos\theta)^2}} d\theta = 2\pi\bar{P} \quad (31)$$

The first term represents the tip resistance which acts throughout the cycle. This term has been reduced by $2\pi\gamma P_0$, the skin friction component, which is normally included when plowing motions that contact uncut soil periodically are considered. The second term represents the frictional resistance to the blade motion, which acts throughout the blade cycle. Nondimensionalizing this equation, and making certain obvious simplifications in the integral, we find

$$(1-\gamma) + \frac{2\gamma\hat{v}}{\pi\sqrt{1+\hat{v}^2}} \int_0^{\pi/2} \frac{d\theta}{\sqrt{1 - \left(\frac{1}{1+\hat{v}^2}\right)\sin^2\theta}} = \hat{p} \quad (32)$$

The integral is the complete elliptic integral of the first kind, denoted by K. The modulus is

$$k = \frac{1}{\sqrt{1+\hat{v}^2}} \quad (33)$$

Thus, for the case of vertical harmonic motion of the plow blade, we have the exact solution

$$(1-\gamma) + \frac{2\gamma\hat{v}}{\pi\sqrt{1+\hat{v}^2}} K\left(\frac{1}{\sqrt{1+\hat{v}^2}}\right) = \hat{p} \quad (34)$$

The elliptic integral is tabulated in numerous references, e.g., reference [5]. Because $\hat{v}$ is normally small, ($0 \leq \hat{v} \leq 0.2$), the modulus in equation (34) is near unity, hence a series expansion

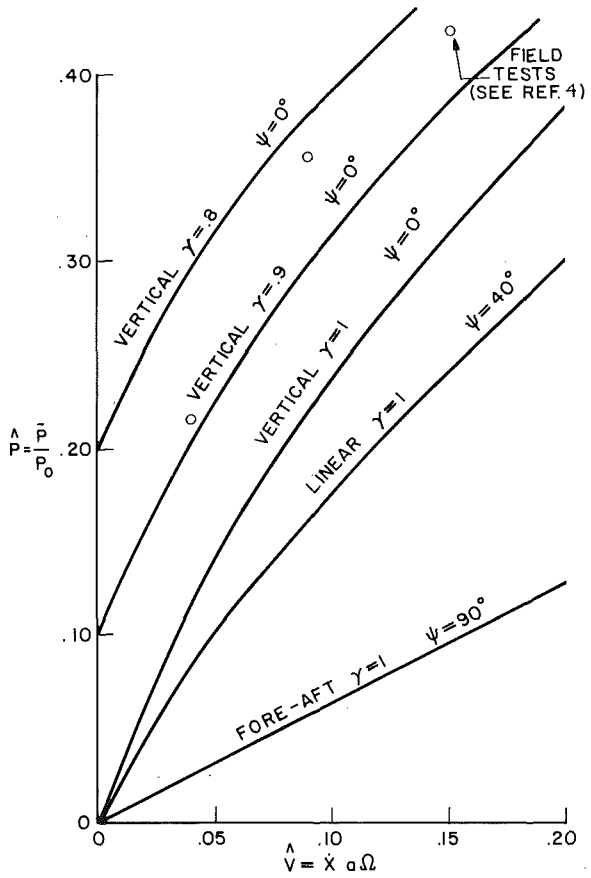

Fig. 5 Bounding solutions and experiment field data for linear vibration

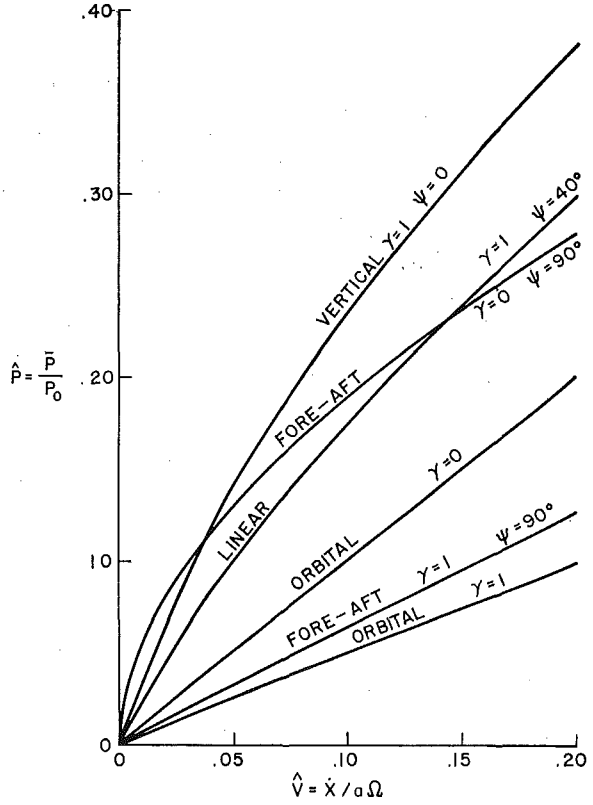

Fig. 6 Bounding solutions for various modes of plow blade vibration

of the function K is extraordinarily cumbersome, requiring far too many terms for any sort of accuracy.

The upper bound for vertical vibration is obtained by setting $\gamma = 0$ or

$$\hat{p} = 1; \quad (\text{all } \hat{v}) \tag{35}$$

This simply represents the static plowing case, as expected. To establish the lower bound, place $\gamma = 1$, and the result is

$$\hat{p} = \frac{2\hat{v}}{\pi\sqrt{1 + \hat{v}^2}} K\left(\frac{1}{\sqrt{1 + \hat{v}^2}}\right) \tag{36}$$

Equation (36) is plotted in Fig. 5. This figure repeats the "all skin friction" fore-aft result from Fig. 4 and shows the numerical result for a general linear harmonic case with $\psi = 40$ deg and $\gamma = 1$. Preliminary field data obtained at Bell Laboratories with vertically vibrating plowing equipment are also shown in this figure.

Discussion of Results

The combined results for the orbital, fore-aft, and vertical vibrating plows are given in Fig. 6. This figure gives a graphic interpretation of the relative merits of each of these modes of vibration.

For a given penetration rate, $\hat{v}$, vertically vibrating plows require the largest average drawbar force. The vertically vibrating plow is essentially a static plow ($\hat{p} = 1$) if $\gamma = 0$. The "all tip resistance" case is approached in practice only if a thick, blunt blade is used. Experimental field data shown in Fig. 5 suggest $\gamma \simeq 0.8$ for more realistic plow geometry, however. The fact that the vertical mode requires the highest drawbar forces is discouraging, because it is the mode of vibration commonly found on commercial utility plows.

Fig. 5 indicates that a substantial decrease in the required drawbar force for linearly vibrating plows can be obtained by increasing ψ. The applied drawbar force decreases monotonically to the limiting case, $\psi = 90$ deg, representing fore-aft vibration. The results show that fore-aft vibration of the plowshare minimizes the required average drawbar force for linear harmonic motion of the blade. Drawbar forces are only 20 to 25 percent of those required with vertical vibration. This reduction is not, however, without penalty. Increased suspension and isolation problems occur with horizontally vibrating equipment.

Orbital motion of a plow blade produces very attractive results. Reductions beyond those available with fore-aft vibration are possible. However, these reductions are also not without cost, for in order to implement this mode of vibration, a "soft-inertial" two-degree-of-freedom suspension system is required. These problems have substantially been solved in an experimental [6, 7] orbital actuator built at Bell Laboratories. This actuator provided the experimental field data plotted in Fig. 3. As in the vertical case, γ near 0.8 seems to be indicated by the experimental data.

Conclusions

This paper presents simple bounds for the reduction in the applied drawbar force required to penetrate soil with vibrating plows. Harmonically forced orbital and linear motions of a plow blade have been investigated. Approximate bounding solutions, which relate applied drawbar force to average plowing speed and other system parameters are obtained for each of these motions. The bounding solutions are simple equations. These results put into perspective the relative merits of each of these motions and compactly express relationships between the important system parameters.

Experimental field data taken at Bell Laboratories show good correlation with the bounding solutions presented. These results suggest that $\gamma \simeq 0.8$ in the Coulomb model adequately predicts vibrating plow performance in the soils at Bell Laboratories' Chester location.

APPENDIX

To solve the transcendental equation (10),

$$2\pi\hat{v} = \cos\alpha - \cos\phi + \hat{v}(\alpha + \phi)$$

first make the change of variable $\phi = 2\pi - \xi$, and then use the expressions for α and $\cos\alpha$ in terms of $\hat{v}$ already given.

$$2\pi\hat{v} = \sqrt{1 - \hat{v}^2} - \cos\xi + \hat{v}^2 + 2\pi\hat{v} - \hat{v}\xi + 0(v^3) \quad (37)$$

or

$$\cos\xi + \hat{v}\xi = 1 + \frac{1}{2}\hat{v}^2 + 0(v^3) \quad (38)$$

For a given value of $\hat{v}$, this is clearly a transcendental equation in ξ, requiring either graphical or numerical solution. Reversing the roles of the two variables, however, it is a quadratic equation in $\hat{v}$, with the immediate solution,

$$\hat{v} = \xi\left\{1 - \sqrt{1 - \frac{2(1 - \cos\xi)}{\xi^2}}\right\} \quad (39)$$

The solution of equation (38) of interest is located near $\xi = 2\pi$. This conclusion follows directly from Fig. 2. The term $2(1 - \cos\xi)/\xi^2$ is therefore small, and equation (39) can be written as

$$\hat{v} \simeq \left(\frac{1 - \cos\xi}{\xi}\right)\left\{1 + \frac{1}{2\xi}\left(\frac{1 - \cos\xi}{\xi}\right) + \ldots\right\}. \quad (40)$$

A numerical comparison of the solutions for $\hat{v}$ given by equations (39) and (40) for 270 deg $\leq \xi \leq$ 360 deg shows that the results agree to three decimal places.

Working with equation (40), we introduce the switching angle ϕ once again.

$$\xi = 2\pi - \phi = 2\pi(1 - \epsilon) \quad (41)$$

where

$$\epsilon = \phi/2\pi \quad (42)$$

is a small parameter. In terms of ϵ, equation (40) becomes, after some algebra,

$$\hat{v} \simeq \pi\epsilon^2\left\{1 + \epsilon + \left(\frac{5}{4} - \frac{1}{3}\pi^2\right)\epsilon^2 + \left(\frac{7}{4} - \frac{1}{3}\pi^2\right)\epsilon^3 \ldots\right\} \quad (43)$$

At this point, we introduce the auxiliary variable η defined by

$$\eta^2 = \frac{\hat{v}}{\pi}, \quad (44)$$

so equation (43) becomes

$$\eta^2 = \epsilon^2\left\{1 + \epsilon + \left(\frac{5}{4} - \frac{1}{3}\pi^2\right)\epsilon^2 + \left(\frac{7}{4} - \frac{1}{3}\pi^2\right)\epsilon^2 \ldots\right\} \quad (45)$$

We now postulate the asymptotic inverse expansion

$$\epsilon = \eta(1 + a\eta + b\eta^2 + c\eta^3 + \ldots) \quad (46)$$

When this expression is substituted into equation (45), the coefficients of ascending powers of η appearing on the right-hand side within the braces are equated to zero. This procedure generates a recursive sequence of equations from which the unknown coefficients $a, b, c \ldots$ may be determined. The result is

$$\epsilon = \eta\left(1 - \frac{1}{2}\eta + \frac{1}{6}\pi^2\eta^2 - \frac{1}{3}\pi^2\eta^3 \ldots\right) \quad (47)$$

Returning to the variables of interest, $\hat{v}$ and ϕ, we have

$$\phi = 2\sqrt{\pi\hat{v}}\left(1 - \frac{1}{2\pi}\sqrt{\pi\hat{v}} + \frac{1}{6}\pi\hat{v} - \frac{1}{3\pi}\pi\hat{v}\sqrt{\pi\hat{v}} \ldots\right) \quad (48)$$

as the asymptotic solution of equation (38).

The solution given by equation (48) differs from the solution expressed by equation (39) by, at most, 2 deg (at ϕ = 90 deg) throughout the range $0 \leq \phi \leq$ 90 deg. The nondimensional penetration rate, $\hat{v}$, corresponding to ϕ = 90 deg is 0.217, establishing an upper bound on this parameter for the purposes of this analysis. For larger values of $\hat{v}$, downward cutting occurs. The solutions developed here remain valid for larger values of $\hat{v}$, although their accuracy begins to deteriorate rapidly. In any case, the larger values of $\hat{v}$ are of little practical interest.

The trigonometric functions of ϕ required in equation (15) are developed using equation (48) and the conventional series expansions for sine and cosine.

References

1 Senator, M. and Warren, R., "Predicting Penetration Rates of Plows With Combined Vertical and Fore-Aft Vibration and Flexible Blades," SAE paper, #7000040 Automotive Engineering Congress, Detroit, Mich., January, 1970.

2 Boyd, R. J., and Nalezny, C. L., "A Model of Vibratory Soil Cutting," SAE Paper 670750, presented at the Farm, Construction, and Industrial Machinery Meeting, Milwaukee, Wis., Sept., 1967.

3 Scerbo, L. J., and Pope, D. L., "The Effects of Upward Cutting on Drawbar Reduction—An Approximate Solution," BTL Memorandum, August 23, 1972.

4 Wells, K. P., "Field Experiments to Determine Relationships Between Blade and Vibration Parameters and Their Effect on Required Drawbar Force," BTL Memorandum, August 21, 1972.

5 Abramowitz, M., and Stegun, I. A., *Handbook of Mathematical Functions*, Chapter 17, National Bureau of Standards, June, 1964.

6 Scerbo, L. J., "Orbital Cable Plow—Design and Test Program for Orbital Actuator," BTL Memorandum, May 13, 1970.

7 Scerbo, L. J., "Orbital Cable Plow—Prospectus for Project," BTL Memorandum, July, 1970.